

1 *Article*

2 **Selecting the most effective DBS contact in essential** 3 **tremor patients based on individual tractography**

4 **Jan Niklas Petry-Schmelzer*¹, Till A. Dembek*¹, Julia K. Steffen¹, Hannah Jergas¹, Haidar S.**
5 **Dafsari¹, Gereon R. Fink^{1,2}, Veerle Visser-Vandewalle³, Michael T. Barbe¹**

6 ¹ University of Cologne, Faculty of Medicine and University Hospital Cologne, Department of Neurology,
7 Germany

8 ² Cognitive Neuroscience, Institute of Neuroscience and Medicine (INM-3), Research Center Jülich, Jülich,
9 Germany

10 ³ University of Cologne, Institute of Medicine and University Hospital Cologne, Department of Stereotactic
11 and Functional Neurosurgery, Germany

12 *These authors contributed equally

13

14 Correspondence: till.dembek@uk-koeln.de; +49 221 478 97602

15 **Abstract:** Postoperative choice of the most effective DBS contact in patients with essential tremor
16 (ET) so far relies on lengthy clinical testing. It has been shown that the postoperative effectiveness
17 of DBS contacts depends on the distance to the dentatorubrothalamic tract (DRTT). Here, we
18 investigated whether the most effective DBS contact could be determined from the stimulation
19 overlap with the individual DRTT. Seven ET patients with bilateral thalamic deep brain stimulation
20 were included retrospectively. Tremor control was assessed contact-wise during test stimulation
21 with 2mA. The individual DRTTs were identified from diffusion tensor imaging. Contacts were
22 ranked by their overlap of the test stimulation with the respective DRTT in relation to their clinical
23 effectiveness. A linear mixed-effects model was calculated to determine the influence of the DRTT-
24 overlap on tremor control. In 92.9 % of the cases, the contact with the best clinical effect was the
25 contact with the highest or second-highest DRTT-overlap. On the group level, the DRTT-overlap
26 explained 26.7% of the variance of the clinical outcome ($p < 0.001$). To conclude, data suggest that the
27 overlap with the DRTT based on individual tractography may serve as a marker to determine the
28 most effective DBS contact in ET patients and reduce burdensome clinical testing in the future.

29 **Keywords:** essential tremor, dentatorubrothalamic tract, volume of tissue activated, deep brain
30 stimulation, tractography, automated programming

31

32 1. Introduction

33 Essential tremor (ET) is the most common adult movement disorder, causes significant
34 disability, interferes with activities of daily living, and reduces quality of life. For medication-
35 refractory cases, deep brain stimulation (DBS) of the thalamic ventral intermediate nucleus (VIM)
36 and the posterior subthalamic area (PSA) is an established effective, and safe treatment [1,2].
37 However, postoperative choice of the most effective contact relies on time-consuming and exhausting
38 clinical testing, especially with new generations of “directional leads” consisting of up to eight
39 contacts.

40
41 DBS most likely modulates pathologic activity within the tremor network via cerebello-thalamo-
42 cortical connections, i.e., the dentatorubrothalamic tract (DRTT) [3]. Additionally, it has been shown
43 that direct targeting of the DRTT leads to successful tremor control and that the effectiveness of a
44 contact depends on its distance to the DRTT [3–6]. We hypothesized that the most effective
45 postoperative contact can be determined in silico by the overlap of the stimulation with the respective
46 DRTT.

47 2. Materials and Methods

48 2.1 Study design

49 This retrospective study included ET patients with bilateral stereotactic DBS lead implantation
50 in PSA/VIM, who had undergone neurosurgery between January 2019 and January 2020, with
51 available preoperative cerebral MRI, diffusion tensor imaging (DTI), and postoperative CT. Patient
52 selection and implantation procedures have been described in detail [2]. All patients were implanted
53 with directional leads (Cartesia™, Boston Scientific, USA). Three months postoperatively, patients
54 underwent routine clinical testing to determine the most effective contact for postoperative tremor
55 control. The study was approved by the local ethics committee (Vote: 20-1511). Due to the
56 retrospective character of the study no informed consent was needed.

57 2.2 Clinical outcome and lead reconstruction

58 As per clinical routine at our center, postural tremor, intention tremor, and rest tremor of the
59 upper limb contralateral to the active stimulation site were assessed without stimulation and during
60 contact-wise stimulation with a fixed amplitude of 2mA, a frequency of 130Hz, a pulse width of 60μs.
61 Contralateral stimulation was switched off during the testing. Clinical scores ranged from 0 (“no
62 tremor”) to 4 (“most severe tremor”). For directional levels, each contact was examined separately.
63 For further analysis, the sum of postural, intention, and rest tremor percentual change scores from
64 the “OFF stimulation” baseline were calculated. DBS leads and their respective rotation were
65 identified from postoperative CT scans, and lead locations were transformed into the preoperative
66 MRI using the Lead-DBS toolbox (www.lead-dbs.org) [7–9]. Respective volumes of tissue activated
67 (VTAs) were calculated in individual patient space using FASTFIELD with an electrical field
68 threshold of 0.2 V/mm and an isotropic conductivity of 0.1 S/m [10,11].

69 2.3 Probabilistic tracking of the DRTT

70 MRI data were acquired on a 3-Tesla Philips Ingenia® Scanner (Philips, Amsterdam, The
71 Netherlands) (T1-sequence: TR: 9.8ms, TE: 4.9ms, acquisition time: 6:13min, voxel-size:
72 0.49x0.49x1.00mm³). For diffusion imaging, a single-shot 2D, spin-echo, echo-planar imaging pulse
73 sequence was applied (TR: 8213ms, TE: 103ms, 40 gradient directions, b-value: 1000s/mm²,
74 acquisition time: 9:53min, voxel-size; 2.0x2.0x2.0mm³). For probabilistic fiber tracking, we used the
75 FMRIB software library (FMRIB, Oxford, UK). We employed probabilistic fiber tracking, as it might
76 be better in detecting the DRTT than the deterministic algorithms embedded in commercially
77 available stereotactic planning software [12]. Diffusion data were corrected for susceptibility-induced
78 distortions using the topup-tool and corrected for head motion and eddy current distortion using the

79 eddy-tool. Brain extraction of the b0-image was performed using the BET-tool, and distributions of
80 diffusion vectors were estimated for each voxel with BEDPOSTX. The number of fibers per voxel was
81 set to two. Probabilistic fiber tracking was performed separately for each DRTT with
82 PROBTRACKX2 using modified Euler integration. For all other parameters, the respective default
83 settings were used. The choice of regions of interest has been described previously [5]. In brief, the
84 contralateral dentate nucleus was chosen as a seed region, while the contralateral superior cerebellar
85 peduncle, the ipsilateral red nucleus, and the ipsilateral precentral gyrus served as waypoints. These
86 regions of interest were previously defined in MNI space and transformed to individual diffusion
87 space using SPM (<http://www.fil.ion.ucl.ac.uk/spm/software/spm12/>) [5]. The resulting track
88 frequency maps were visually examined for anatomical accuracy and transformed into a track
89 probability map, according to Schlaier et al. [12]. Finally, the resulting fiber tracts were coregistered
90 to the preoperative T1.

91 *2.4 Statistical analysis*

92 For further analysis, the overlap of each 2mA VTA with the respective DRTT was calculated as
93 the sum of the resulting track probability map values covered by the respective VTA, multiplied with
94 the VTA's voxel-size in mm³. These DRTT-overlap values were ranked hemisphere-wise to determine
95 the contact with the largest DRTT-overlap. We then investigated how often the electrodes with the
96 highest and second-highest overlap also had the best clinical outcome during clinical testing.
97 Additionally, a linear mixed-effects model was employed to determine the predictive value of the
98 overlap with the individual DRTT regarding tremor control on the group level. We included "DRTT
99 overlap" as the main effect and "lead" as a random-effect, to take multiple testing per lead into
100 account. [13].

101 *2.5 Data availability*

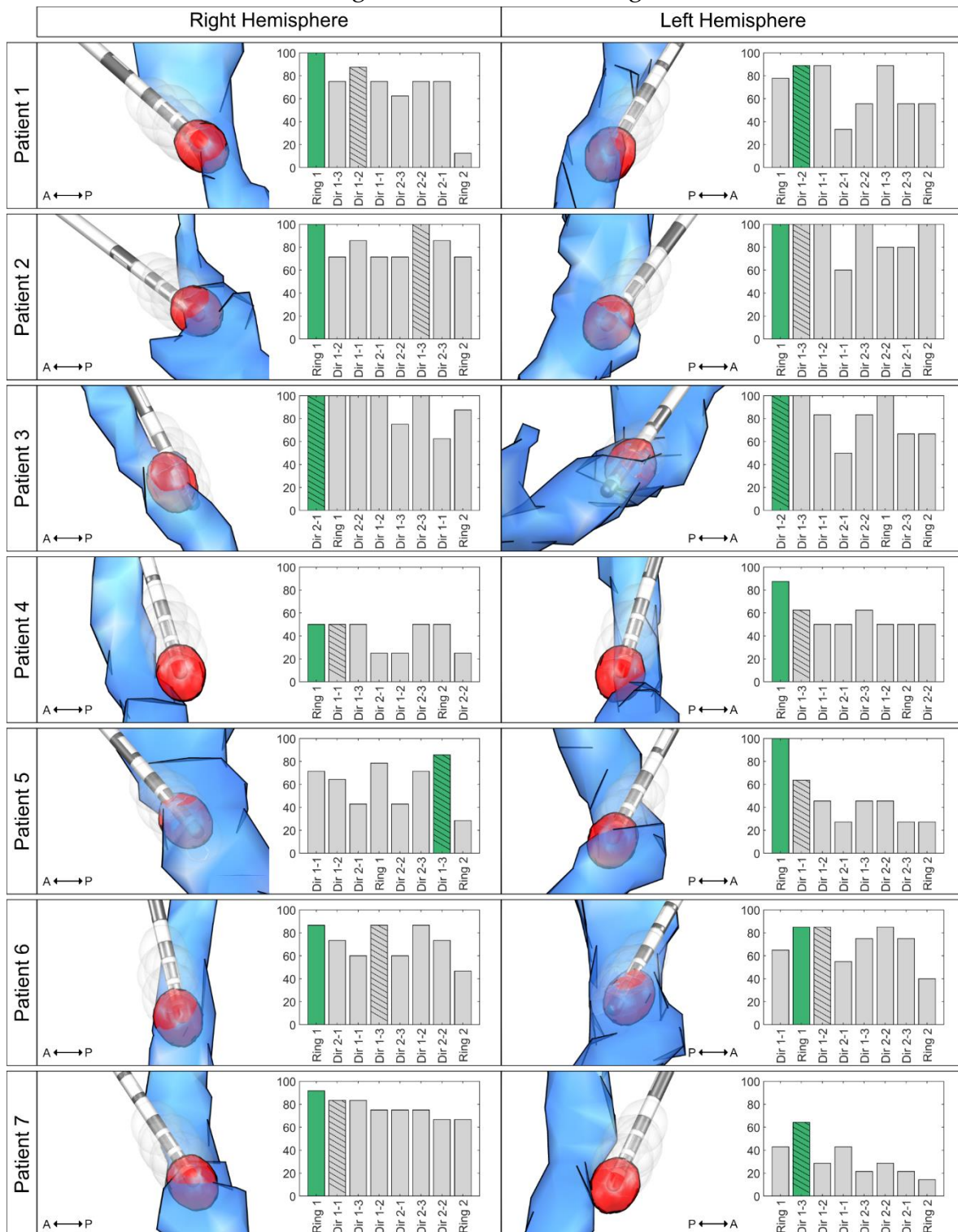
102 Matlab scripts are available from the open science framework (Link follows on acceptance).
103 Anonymized imaging and clinical data are available upon request to the corresponding author and
104 not publicly available due to privacy concerns.

105 **3. Results**

106 A total of 7 ET patients (3 female, age: 68.8 y ±14.8) and 14 directional DBS leads were included
107 in this retrospective analysis. The contact ranking results by clinical effectiveness and overlap with
108 the individual DRTT are shown in Figure 1. In 71.4 % of the cases (10 of 14 hemispheres), the contact
109 with the highest overlap with the individual DRTT showed the best clinical outcome or was among
110 those with the best outcome if more than one contact showed equal tremor improvement. In the
111 remaining cases, in 3 of 4 hemispheres the contact with the second-highest overlap with the
112 individual DRTT showed the best clinical outcome. When only investigating directional contacts, in
113 64.3 % of the cases the directional contact with the highest DRTT-overlap also had the best tremor
114 improvement. On the group level, the linear mixed-effects model explained 68.4% of the variance of
115 clinical outcome, while the overlap with the individual DRTT alone (main-effect) explained 26.7% of
116 the variance ($R^2_{\text{model}} = 0.684$, $R^2_{\text{main-effect}} = 0.267$, $p < 0.001$, see Figure 2). A positive relationship between
117 DRTT-overlap and tremor improvement was observed in all hemispheres.

118

Figure 1 – Contact Ranking



119

120

121

122

123

124

125

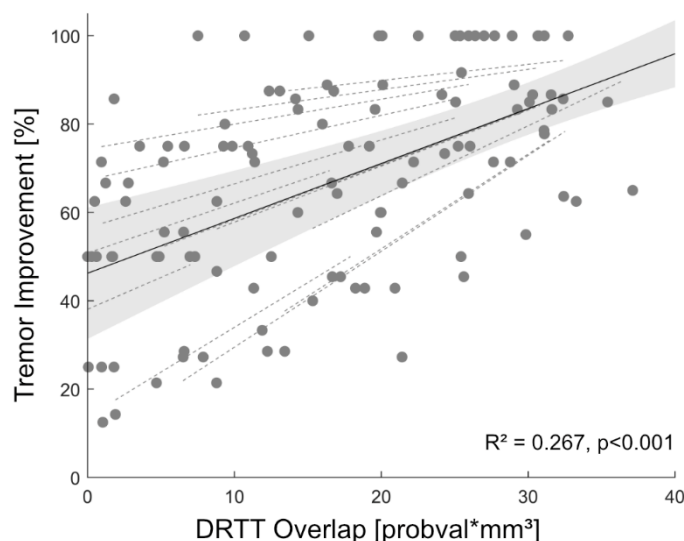
126

127

Figure 1 – Contact Ranking. Bar plots illustrate the ranking of the overlap with the individual dentatorubrothalamic tract (DRTT) per contact on the x-axis (highest overlap to lowest overlap) and the improvement in tremor control in % on the y-axis. The most effective contact is marked in green (with the highest overlap in case more than one contact had the best improvement), and the bar of the most effective directional contact is hatched. The respective left column illustrates the relation of the generated volumes of tissue activated (VTAs, gray) together with the DRTT (blue) and the respective lead in the medial view. The VTA with the highest DRTT-overlap is highlighted in red. For illustration, only the 10% highest values of the track probability map are shown.

128 **Abbreviations:** A = anterior, DRTT = dentatorubrothalamic tract, P = posterior, VTA = volume of
129 tissue activated, Dir 1 = ventral directional level, Dir 2 = dorsal directional level.

130 **Figure 2 – Prediction of Tremor Improvement**



131
132 **Figure 2 – Prediction of Tremor Improvement.** Linear mixed-effects model (black) and 95%
133 confidence interval (gray) between tremor improvement and overlap with the individual
134 dentatorubrothalamic tract (DRTT). Random effects for each individual hemisphere are also shown
135 (dashed, gray). **Abbreviations:** DRTT=dentatorubrothalamic tract.

136 4. Discussion

137 This study demonstrates that the overlap with the DRTT might serve as a marker for in silico
138 determination of the most effective contact for tremor suppression in ET patients. The overlap with
139 the DRTT determined one of the most effective contacts in 71.4%. When also considering the contact
140 with the second-most overlap, this figure increased to 92.9% of the cases. In other words, if one had
141 only interrogated the two contacts with the highest DRTT-overlap, a contact with an optimal outcome
142 would have been determined in 13/14 hemispheres. In the remaining hemisphere (Patient 5, right
143 hemisphere) in which the most effective contact ranked worse, i.e., in seventh place, the contact with
144 the highest overlap still was on the same directional level as the most effective contact and improved
145 tremor by 75%. With new generations of DBS leads, there is the option of steering the current towards
146 more effective contacts, away from contacts causing side effects [14]. Only considering directional
147 contacts, the chance of activating the most effective directional contact without clinical testing
148 increases from 16.7% (1 out of 6) to 64.3% when using the in silico approach presented here.

149 Although landmark-based targeting was used when implanting our patients [2], in the majority
150 of cases, the most ventral contact was the most effective contact with the highest overlap to the DRTT.
151 This finding is in line with previous studies indicating that (i) effective contacts are located inside or
152 close to the DRTT and [3,5] (ii) that in our targeting approach, contacts in the PSA are closer to the
153 DRTT [5]. While there was a positive relationship between DRTT-overlap and tremor suppression in
154 all hemispheres in our mixed-effects model, and overlap predicted 26.7% of the variance in tremor
155 outcome, there were still marked individual differences between hemispheres, as indicated by the
156 68% of variance explained when also considering hemisphere as a random effect.

157 Several attempts to predict postoperative tremor suppression focused on connectivity analysis
158 or probabilistic stimulation mapping [15–17]. However, only Åström et al. [18] focused on predicting
159 the DBS contact to be chosen postoperatively. Based on probabilistic stimulation maps, the resulting
160 software tool, showed that the predicted contact with rank 1 matched the clinically used contact in

161 60% of cases (rank 1-2 matched 83% of the cases). In contrast, the present study was based on the
162 individual DRTT as a neuroanatomical correlate of tremor suppression and included leads with eight
163 contacts instead of four contacts.

164 This study's major limitation is that we only investigated tremor suppression and did not
165 consider stimulation-induced side effects. In several cases, more than one contact showed equally
166 optimal tremor suppression. In such cases, side effect thresholds would be crucial for determining
167 the contact used for clinical stimulation. Therefore, more research regarding the neuroanatomical
168 origins of different stimulation-induced side effects [19] is needed. Prospective studies, also taking
169 stimulation-induced side effects such as muscle contractions, paresthesia, ataxia, and stimulation-
170 induced dysarthria into account, should be conducted to validate and extend this retrospective
171 analysis.

172 Nevertheless, our study demonstrates how in silico imaging analysis could guide clinical DBS
173 programming in ET and help reduce patient burden by shortening tedious monopolar review
174 investigations.

175
176

177 **Supplementary Materials:** None.

178 **Author Contributions:** Conceptualization, JNPS and TAD.; methodology, JNPS and TAD; software, JNPS and
179 TAD.; validation, JNPS and TAD; formal analysis, JNPS and TAD; investigation, JNPS and TAD; resources, JKS,
180 HJ, and VVV; data curation, JNPS and TAD; writing—original draft preparation, JNPS and TAD.; writing—
181 review and editing, JKS, HJ, HSD, GRF, VVV, and MTB; visualization, JNPS and TAD.; supervision, HSD, VVV
182 and MTB; project administration, GRF, VVV and MTB.. All authors have read and agreed to the published
183 version of the manuscript.

184 **Funding:** Supported by the Cologne Clinician Scientist Program (CCSP) / Faculty of Medicine / University of
185 Cologne. Funded by the German Research Foundation (DFG, FI 773/15-1).

186 **Acknowledgments:** None

187 **Conflicts of Interest:** The authors declare no conflict of interest. The funders (Cologne Clinician Scientist
188 Program; German Research Foundation) had no role in the design of the study; in the collection, analyses, or
189 interpretation of data; in the writing of the manuscript, or in the decision to publish the results.

190 **Appendix A**

191 None.

192

193 **Appendix B**

194 None.

195 **References**

- 196 1. Schuurman, P.R.; Bosch, D.A.; Bossuyt, P.M.; Bonsel, G.J.; van Someren, E.J.; de Bie, R.M.; Merkus, M.P.;
197 Speelman, J.D. A comparison of continuous thalamic stimulation and thalamotomy for suppression of
198 severe tremor. *N. Engl. J. Med.* **2000**, *342*, 461–468, doi:10.1056/NEJM200002173420703.
- 199 2. Barbe, M.T.; Reker, P.; Hamacher, S.; Franklin, J.; Kraus, D.; Dembek, T.A.; Becker, J.; Steffen, J.K.; Allert,
200 N.; Wirths, J.; et al. DBS of the PSA and the VIM in essential tremor: A randomized, double-blind,
201 crossover trial. *Neurology* **2018**, *91*, e543–e550, doi:10.1212/WNL.0000000000005956.
- 202 3. Coenen, V.A.; Allert, N.; Paus, S.; Kronenbürger, M.; Urbach, H.; Mädler, B. Modulation of the cerebello-
203 thalamo-cortical network in thalamic deep brain stimulation for tremor: a diffusion tensor imaging study.
204 *Neurosurgery* **2014**, *75*, 657–669; discussion 669-670, doi:10.1227/NEU.0000000000000540.

- 205 4. Fenoy, A.J.; Schiess, M.C. Deep Brain Stimulation of the Dentato-Rubro-Thalamic Tract: Outcomes of
206 Direct Targeting for Tremor. *Neuromodulation* **2017**, *20*, 429–436, doi:10.1111/ner.12585.
- 207 5. Dembek, T.A.; Petry-Schmelzer, J.N.; Reker, P.; Wirths, J.; Hamacher, S.; Steffen, J.; Dafsari, H.S.; Hövels,
208 M.; Fink, G.R.; Visser-Vandewalle, V.; et al. PSA and VIM DBS efficiency in essential tremor depends on
209 distance to the dentatorubrothalamic tract. *Neuroimage Clin* **2020**, *26*, 102235, doi:10.1016/j.nicl.2020.102235.
- 210 6. Chazen, J.L.; Sarva, H.; Stieg, P.E.; Min, R.J.; Ballon, D.J.; Pryor, K.O.; Riegelhaupt, P.M.; Kaplitt, M.G.
211 Clinical improvement associated with targeted interruption of the cerebellothalamic tract following MR-
212 guided focused ultrasound for essential tremor. *J. Neurosurg.* **2018**, *129*, 315–323,
213 doi:10.3171/2017.4.JNS162803.
- 214 7. Horn, A.; Li, N.; Dembek, T.A.; Kappel, A.; Boulay, C.; Ewert, S.; Tietze, A.; Husch, A.; Perera, T.;
215 Neumann, W.-J.; et al. Lead-DBS v2: Towards a comprehensive pipeline for deep brain stimulation
216 imaging. *Neuroimage* **2019**, *184*, 293–316, doi:10.1016/j.neuroimage.2018.08.068.
- 217 8. Dembek, T.A.; Hoevels, M.; Hellerbach, A.; Horn, A.; Petry-Schmelzer, J.N.; Borggreffe, J.; Wirths, J.;
218 Dafsari, H.S.; Barbe, M.T.; Visser-Vandewalle, V.; et al. Directional DBS leads show large deviations from
219 their intended implantation orientation. *Parkinsonism Relat. Disord.* **2019**, *67*, 117–121,
220 doi:10.1016/j.parkreldis.2019.08.017.
- 221 9. Husch, A.; V Petersen, M.; Gemmar, P.; Goncalves, J.; Hertel, F. PaCER - A fully automated method for
222 electrode trajectory and contact reconstruction in deep brain stimulation. *Neuroimage Clin* **2018**, *17*, 80–89,
223 doi:10.1016/j.nicl.2017.10.004.
- 224 10. Baniasadi, M.; Proverbio, D.; Gonçalves, J.; Hertel, F.; Husch, A. FastField: An open-source toolbox for
225 efficient approximation of deep brain stimulation electric fields. *NeuroImage* **2020**, *223*, 117330,
226 doi:10.1016/j.neuroimage.2020.117330.
- 227 11. Astrom, M.; Diczfalusy, E.; Martens, H.; Wardell, K. Relationship between neural activation and electric
228 field distribution during deep brain stimulation. *IEEE Trans Biomed Eng* **2015**, *62*, 664–672,
229 doi:10.1109/TBME.2014.2363494.
- 230 12. Schlaier, J.R.; Beer, A.L.; Faltermeier, R.; Fellner, C.; Steib, K.; Lange, M.; Greenlee, M.W.; Brawanski, A.T.;
231 Anthofer, J.M. Probabilistic vs. deterministic fiber tracking and the influence of different seed regions to
232 delineate cerebellar-thalamic fibers in deep brain stimulation. *European Journal of Neuroscience* **2017**, *45*,
233 1623–1633, doi:10.1111/ejn.13575.
- 234 13. Dembek, T.A.; Roediger, J.; Horn, A.; Reker, P.; Oehr, C.; Dafsari, H.S.; Li, N.; Kühn, A.A.; Fink, G.R.;
235 Visser-Vandewalle, V.; et al. Probabilistic Sweetspots Predict Motor Outcome for DBS in Parkinson's
236 Disease. *Ann. Neurol.* **2019**, doi:10.1002/ana.25567.
- 237 14. Dembek, T.A.; Reker, P.; Visser-Vandewalle, V.; Wirths, J.; Treuer, H.; Klehr, M.; Roediger, J.; Dafsari, H.S.;
238 Barbe, M.T.; Timmermann, L. Directional DBS increases side-effect thresholds—A prospective, double-
239 blind trial. *Movement Disorders* **2017**, *32*, 1380–1388, doi:10.1002/mds.27093.
- 240 15. Akram, H.; Dayal, V.; Mahlknecht, P.; Georgiev, D.; Hyam, J.; Foltynie, T.; Limousin, P.; De Vita, E.;
241 Jahanshahi, M.; Ashburner, J.; et al. Connectivity derived thalamic segmentation in deep brain stimulation
242 for tremor. *Neuroimage Clin* **2018**, *18*, 130–142, doi:10.1016/j.nicl.2018.01.008.
- 243 16. Al-Fatly, B.; Ewert, S.; Kübler, D.; Kroneberg, D.; Horn, A.; Kühn, A.A. Connectivity profile of thalamic
244 deep brain stimulation to effectively treat essential tremor. *Brain* **2019**, *142*, 3086–3098,
245 doi:10.1093/brain/awz236.

- 246 17. Dembek, T.A.; Barbe, M.T.; Åström, M.; Hoevens, M.; Visser-Vandewalle, V.; Fink, G.R.; Timmermann, L.
247 Probabilistic mapping of deep brain stimulation effects in essential tremor. *Neuroimage Clin* **2016**, *13*, 164–
248 173, doi:10.1016/j.nicl.2016.11.019.
- 249 18. Åström, M.; Samuelsson, J.; Roothans, J.; Fytagoridis, A.; Ryzhkov, M.; Nijlunsing, R.; Blomstedt, P.
250 Prediction of Electrode Contacts for Clinically Effective Deep Brain Stimulation in Essential Tremor.
251 *Stereotact Funct Neurosurg* **2018**, *96*, 281–288, doi:10.1159/000492230.
- 252 19. Béreau, M.; Kibleur, A.; Bouthour, W.; Tomkova Chaoui, E.; Maling, N.; Nguyen, T.A.K.; Momjian, S.;
253 Vargas Gomez, M.I.; Zacharia, A.; Bally, J.F.; et al. Modeling of Electric Fields in Individual Imaging Atlas
254 for Capsular Threshold Prediction of Deep Brain Stimulation in Parkinson’s Disease: A Pilot Study. *Front.*
255 *Neurol.* **2020**, *11*, doi:10.3389/fneur.2020.00532.
256